IEEE Access
Multidisciplinary | Rapid Review | Open Access Journal

Received September 13, 2018, accepted October 15, 2018, date of publication October 22, 2018,
date of current version November 14, 2018.

Digital Object Identifier 10.1109/ACCESS.2018.2876919

Imaging Cellular Structures of Atherosclerotic Coronary Arteries Using Circumferentially Scanning Micro-Optical Coherence Tomography Fiber Probe *Ex Vivo*

YUEMEI LUO[1], EN BO[1], HAITAO LIANG[1], XIANGHONG WANG[1], XIAOJUN YU[2], DONGYAO CUI[1], XIN GE[1], JIANHUA MO[3], AND LINBO LIU[1,4]

[1]School of Electrical and Electronic Engineering, Nanyang Technological University, Singapore 639798
[2]School of Automation, Northwestern Polytechnical University, Xi'an 710072, China
[3]School of Electronic and Information Engineering, Soochow University, Suzhou 215006, China
[4]School of Chemical and Biomedical Engineering, Nanyang Technological University, Singapore 637459

Corresponding author: Linbo Liu (liulinbo@ntu.edu.sg)

This work was supported in part by the National Research Foundation Singapore under Grant NRF-CRP13-2014-05, in part by the National Natural Science Foundation of China under Grant 61705184, in part by the National Natural Science Foundation of China under Grant 81401451, in part by the Ministry of Education Singapore under Grant MOE2013-T2-2-107, in part by the National Medical Research Council Singapore under Grant NMRC/CBRG/0036/2013, and in part by the NTU-AIT-MUV Program in Advanced Biomedical Imaging under Grant NAM/15005.

ABSTRACT Development and progression of coronary atherosclerotic lesions is mediated by a number of cellular components that are not readily visualized using the current clinical investigation tools. Visualizing these cellular components in situ and in vivo may allow early detection of the vulnerable plaques, with implications for coronary artery disease therapy and for the prevention of acute myocardial infarction. In this paper, we have developed a fiber-optic micro-optical coherence tomography (μ OCT) probe for intravascular use. We conducted *ex vivo* imaging experiments in normal swine aorta and human atherosclerotic coronary arteries and demonstrated that the fiber-probe-based μ OCT could delineate not only the layered structures of arterial wall but also the cellular-level anatomical structures of atherosclerotic plaques, including foam cells and smooth muscle cells. These results demonstrate the feasibility of intravascular μ OCT imaging.

INDEX TERMS Optical fiber devices, optical coherence tomography, fiber optics imaging, intravascular imaging.

I. INTRODUCTION

Coronary artery disease (CAD) is one of the leading causes of global morbidity and mortality, and its clinical manifestation, acute myocardial infarction (AMI), often commonly caused by the rupture or erosion of atherosclerotic plaques [1]–[3]. If vulnerable sites can be detected before rupture or erosion, effective intervention and medical treatments could be adopted to prevent clinical events, and herein, identification of high-risk lesions before worst situations is of great importance. Thin-cap fibroatheroma (TCFA), a lesion served as a predecessor of vulnerable plaques, has been characterized as plaques with a thin fibrous cap (less than 65 μm in thickness) together with macrophages infiltration near or within the cap, and a large lipid pool [4], [5]. Specifically, development and progression of atherosclerotic lesions is mediated by a number of cellular compositions including smooth muscle cells and accumulation of fat-laden foam cells or macrophages [3], [6]. Therefore, quantification of these cellular compositions can assist to assess the plaque vulnerability at an early stage.

Computerized tomography (CT) and magnetic resonance imaging (MRI) are commercially utilized for non-invasive atherosclerotic plaque screening with a spatial resolution in the order of hundreds of micrometers [7]. Intravascular ultrasound (IVUS) with a resolution of 70-100 μm is clinically developed to characterize plaques [8], [9]. Optical coherence tomography (OCT), another non-invasive imaging modality, has recently been proposed to image microstructures of coronary artery [10]. Particularly, intravascular OCT (IVOCT) with approximately $\sim$7 μm axial resolution

in tissue and ∼20-30 μm transverse resolution, which is able to visualize the fibrous cap, macrophages infiltration and lipid pool, is emerged to investigate *in vivo* visualization of the microstructural features of coronary atherosclerotic plaques [11]–[13]. These technical advances have significantly improved the diagnostic outcome of TCFA. However, further improvement on the early detection of atherosclerotic lesions based on the visualization of cellular compositions is limited by the spatial resolution of the available imaging technologies.

To tackle this issue, OCT with sub-micrometer resolution has been reported for imaging [14], [15], while there is still not equipped with a flexible and miniature probe. Recently, a new generation of OCT technology, termed micro-optical coherence tomography (μ OCT), is capable of delineate microstructure with 1-4 μm spatial resolution and become promising to capture cellular characteristics for atherosclerotic plaque detection [16]–[19]. In particular, both a rigid and a flexible μ OCT endobronchial probe were reported for airway imaging *in vivo* by linear scanning [18], [20]. However, no progress has been made for intravascular imaging by circumferentially scanning μ OCT probe. In this paper, we applied a flexible and circumferentially scanning μ OCT probe for intravascular imaging to acquire the cellular compositions by conducting *ex vivo* imaging experiments in normal swine aorta and human atherosclerotic coronary arteries, and testified its feasibility toward clinical translation. It is the first time, to the best of our knowledge, to verify the capability of fiber-probe based μ OCT for visualizing microstructures of coronary artery at the cellular level.

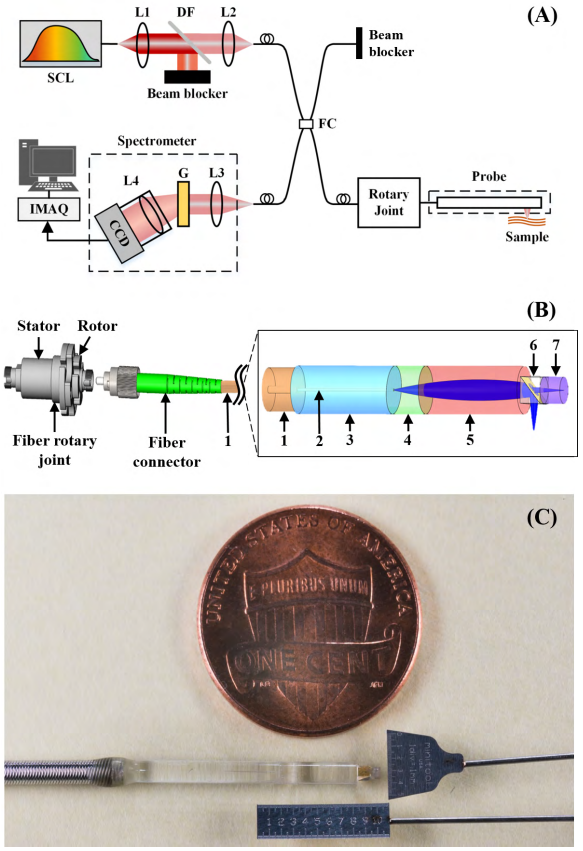

FIGURE 1. (A) Schematic of the fiber-probe based μ OCT system. SCL: supercontinuum light source; DF: dichroic filter; L1-L3: achromatic lens; FC: fiber coupler; G: grating; L4: camera lens; IMAQ: imaging acquisition. (B) 3-D configuration of the probe together with the fiber rotary joint. 1: driveshaft; 2: single mode fiber; 3: ferrule; 4: glass spacer; 5: GRIN lens; 6: beamsplitter; 7: reference reflector. (C) Photograph of the fabricated probe compared with a one-cent coin.

II. MATERIALS AND METHODS

A. FIBER-PROBE BASED μ OCT

The construction of the fiber-probe based μ OCT system used in this study is shown in Fig. 1(A), including an imaging console and a common-path fiber-optic probe for beam delivery toward the sample, and the details have been previously reported in [21]. Briefly, the system applied a broadband light source centered at ∼800 nm with ∼250 nm spectral range full width at half maximum (FWHM) by a supercontinuum light source (Superk Extreme OCT; NKT Photonics, Birkerød, Denmark) together with a following short pass dichroic filter (DMSP1000; Thorlabs Inc., Newton, New Jersey, USA). A fiber coupler (Gould Fiber Optics, Millersville, Maryland, USA) with a splitting ratio of 50:50 was utilized to direct the light source toward the probe via a rotary joint. The rotary joint consists of a rotation stage (URB100CC; Newport, Irvine, California, USA) with a speed of 360ř/second and a fiber rotary joint (Princetel Inc., Hamilton Township, New Jersey, USA) for the rotation transmission from the motor to the probe. Indicated as the Fig. 1(B), the fiber rotary joint consists of two parts: one is the stator which is connected to the output port of fiber coupler to deliver the beam, while the other is the rotor which can be rotated by connecting to a rotation motor (not shown in this figure). During the imaging, the rotor is connected to a fiber connector (30126A3; Thorlabs Inc.), which is glued to the probe via a flexible torque-coil driveshaft (Asahi Intecc Co., Japan.), and therefore, the fiber connector can transmit the rotation motion to the probe via the driveshaft to conduct the circumferential scanning. In this study, we developed a new fiber-optic probe by upgrading a previously reported design with a torque-coil driveshaft, which enabled intravascular imaging in intact coronary arteries.

Depicted as probe configuration highlighted as the black box in Fig. 1(B), in the illumination path, after transmitted by a single-mode fiber (SMF) (780HP; Thorlabs Inc.), the beam was then expanded by a BK7 glass spacer with a diameter of 1.8 mm and a length of 1.63±0.07 mm (GrinTech GmbH, Jena, Germany) and then focused by a gradient-index (GRIN) lens (GT-LFRL-180-50; GrinTech GmbH) with a diameter of 1.8 mm and a length of 4.991 mm. After that, a beamsplitter (BS), comprised of two right angle prisms (Changchun Boxin Photoelectric Co., Changchun, China) with an apodizing coating in between, was used to divide the beam into a center circular beam and an annular beam.

The center circular beam as the reference beam was guided to a glass rod (Prime Bioscience, Singapore) with a length of 0.80 ± 0.02 mm and a gold coating on its end surface to reflect the beam, while the annular beam as the sample beam was redirected by 90ř outside to the imaging sample and then backscattered, similar to the previous studies in [16], [18]. The beam with annular configuration acts as a phase pupil filter to generate a moderately extended depth-of-focus (DOF) with a maintained transverse resolution [16], [18], [22]. The incident power for the sample was measured as 12.8 mW. In the detection path, the reflected beam and backscattered beam interfered and returned along the same path into the SMF.

During the imaging, a transparent outer sheath tube (51-2800-1800; Thorlabs Inc.) was served as a barrier to protect imaging tissues from rotating probe. Besides, the inner diameter (ID) of 1.818 mm of the sheath and the diameter of 1.8 mm of the optical probe forms a clearance fit so that the probe can rotate freely and co-axially with the sheath. For the outer diameter (OD) of the sheath, it is designed as 2.8 mm to fully fill the luminal area so that imaging tissues are positioned within the optimal imaging range to ensure area of interests properly maintained around the focal region.

The interferometric signal returning from the probe was then guided into a spectrometer including an achromatic lens (AC127-030-B-ML; Thorlabs Inc.), a diffractive grating with 960 lines/mm at 840 nm (Wasatch Photonics Inc., Logan, Utah, USA), a camera lens (Nikon AF Nikkor 85 mm f/1.8D; Tokyo, Japan) and a line-scan CCD camera (E2V, AViiVA EM4-EV71YEM4CL2014-BA9) to detect the signal. The detected spectrum was then digitalized at a 12-bit resolution and transferred to computer through an imaging acquisition (IMAQ) card (KBN-PCECL4-F; Bitflow Inc., Woburn, Massachusetts, USA) and a camera link cable. At the meanwhile, the computer generates a triggering signal of 20 kHz to synchronize the camera, and consequently, the system scanning rate was 20 k lines/second. During image post-processing, 2-frame averaging (time-lapse averaging) and software based speckle reduction [23], [24] were conducted to reduce the image speckle and thus improve the cellular-level imaging contrast.

B. SYSTEM PERFORMANCE

To testify the system axial resolution, we placed a glass surface with a reflectivity of 4% at the focus. The axial point spread function (PSF) in Fig. 2(A) demonstrated the axial resolution of 2.1 μm in air, and correspondingly of 1.53 μm in tissue assuming the refractive index of 1.37. To verify the transverse resolution, a laser beam profiler (LBP2-HR-VIS2; Newport) and an objective (50× DRY Plan Fluorite Objective; Nikon) were applied to capture the sample beam, and the results in Fig. 2(B) shown that the transverse resolution was measured to be 4.8 μm at the focus (assuming the depth of 0 μm). DOF represents the axial distance over which the beam size at the $1/e^2$ beam is not larger than 1.414 times of that at the beam waist. As illustrated in Fig. 2(B), compared

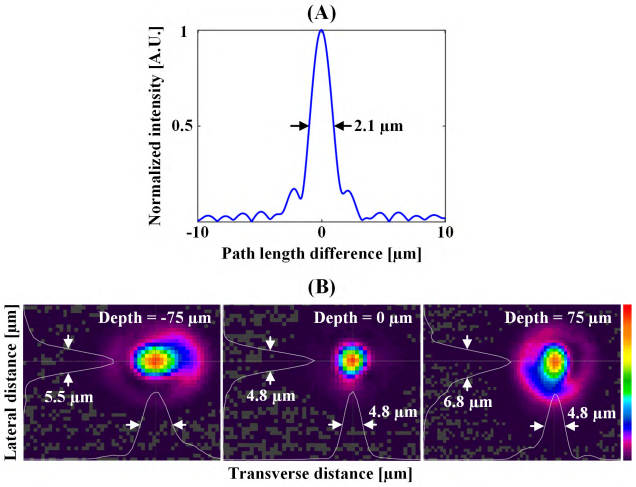

FIGURE 2. (A) Measured axial point spread function (PSF) of the system. (B) Two-dimensional images of the spot at the focus (depth = 0 μm) and other 2 axial depths by the beam profile. Lateral profiles and transverse profiles are displayed in left and bottom sides, respectively. The beam was measured in air and without the glass outer sheath. Intensity is scaled in color bar and it is in linear scale.

to the focused spot (depth = 0 μm), the spot size almost becomes 1.414 time larger at ± 75 μm away for the focal plane, and herein the DOF was measured as ∼150 μm. The irregularity of intensity distribution in Fig. 2(B) was caused by the fabrication defects in annular gold coating on the BS.

C. IMAGING PROCEDURES

We collected freshly explanted swine aorta tissues from a slaughterhouse in Singapore. Fresh human atherosclerotic coronary artery tissues were extracted from a cadaver heart. The blood vessels were flushed by phosphate buffered saline (PBS) solution to remove the blood debris, and during the experiments, we also applied the PBS to fill in the blood vessels. We inserted the probe together with outer sheath into the coronary artery lumen so that the imaging tissues surround the outer surface of sheath tightly. In addition, when finishing image acquisition, the human coronary artery tissues were fixed using 4% neutral buffered formaldehyde and then stained using hematoxylin and eosin (H&E) for histological analysis in comparison with μ OCT images.

The study using human arterial tissues was approved by the Institutional Review Board at Nanyang Technological University (IRB-2014-12-004). The study using animal was approved by the Institutional Animal Care and Use Committee (IACUC) of Nanyang Technological University, Singapore (ARF-SBS/NIE-A0312).

To estimate the high resolution of this fiber-probe based μ OCT, we compared the obtained μ OCT images with the corresponding images simulated by a ∼7 μm axial resolution in tissue and a ∼20 μm transverse resolution which is the highest resolution of current OCT for intracoronary imaging to date [11]–[13]. This simulation was achieved by two steps: the first step is to apply two Gaussian-shape coherence

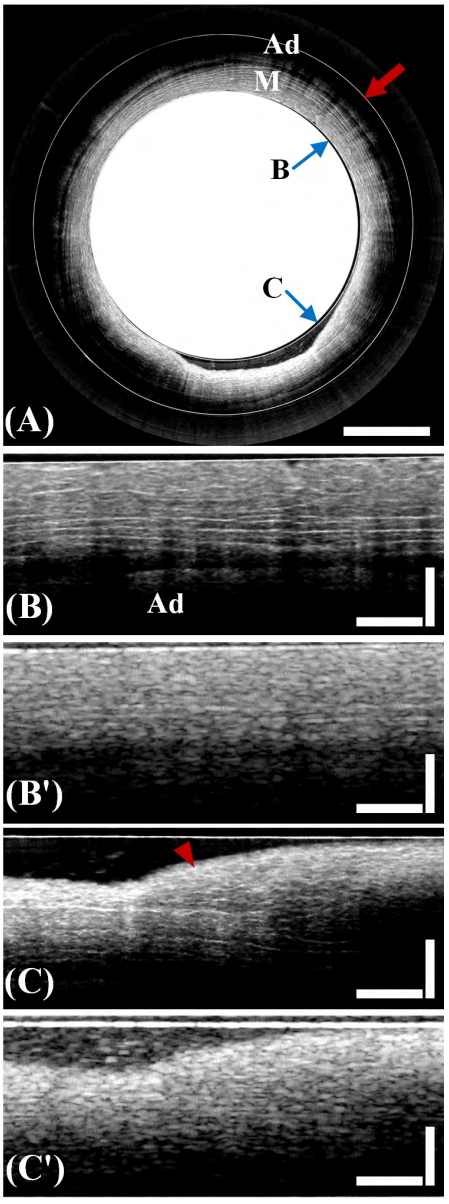

FIGURE 3. Cross-sectional images of a normal swine aorta *ex vivo*. (A) A representative cross-sectional μ OCT image during circumferential scanning showing anatomical information of media (M), adventitia (Ad) and internal elastic lamina (IEL). It consists of 1024 pixels (axial, 1016.8 μm) × 5188 pixels (circumferential, minimum circle: 8375.5 μm). (B) Magnified view indicating the multiple signal-rich elastic laminas and alternative signal-poor smooth muscle within the media. (C) Magnified view depicting the signal-rich IEL as a thin hyper-reflective band just beneath the inner luminal surface of tissues (red arrow head), and the underlying multiple elastic lamina and smooth muscle within the media. (B′, C′) Simulated images by OCT with an axial resolution of ∼7 μm in tissue and a transverse resolution of ∼20 μm corresponding to the obtained visualizing results in (B, C), respectively. Image size of (B, C): 637.5 μm (axial) × 1259.5 μm (circumferential). Red arrow in (A) indicates the conjugated profile of the inner surface of outer sheath. Scale bars: 1 mm in (A); 200 μm in (B, C).

functions with an axial FWHM of ∼7 μm in tissue and a transverse FWHM of ∼20 μm to convolute with our detected imaging data, respectively; then the second step is to combine the above convoluted results.

III. RESULTS AND DISCUSSION

In a representative cross-sectional μ OCT image (Fig. 3(A)), layers of media and adventitia can be clearly distinguished. Additionally, shown as Figs. 3(B, C), within the media, both the circumferentially oriented elastic laminas with high reflectivity and alternative low-scattered smooth muscle can be frequently and evidently observed in regular arrangement.

The internal elastic lamina (IEL), a layer of elastic tissue as the outermost part of the thin intima, is a flexible barrier between the arterial intimal and medial layers, and it may have an effect on atherosclerosis via its modulation of diffusion across the artery wall [25]. By imaging the normal swine aorta, regular IEL is acquired as a bright and very thin structure (Fig. 3(C)).

Previous histopathological studies have revealed that atherosclerotic plaque progression is commonly featured by grossly thickened intima and irregular layered structures [25]. The μ OCT image of human atherosclerotic plaque (Fig. 4) illustrates the cross-section of arterial wall with intimal thickening, in accordance with the histopathological characteristics.

Foam cells, usually appeared as fat-laden engorged macrophages, serve as a hallmark of plaque build-up and atherosclerosis formation [16], [26]–[28]. In a μ OCT image (Fig. 4(D)), the foam cells derived from macrophages can be evidently resolved and the accumulation of these foam cells is manifested as clusters of punctate highly-scattering spots. The corresponding histological findings (Fig. 4(D), bottom inset) present a consensus on the μ OCT images. Besides, we also visualized another foam cells with similar scattering intensity of aforementioned foam cells but with spindle shape, which may be derived from smooth muscle cells (Fig. 4(C)).

Within the progression of atherosclerotic plaque, smooth muscle cells migrate and proliferate from the media into the intima [3], [6], [25], [29]. In μ OCT images, smooth muscle cells can be visualized as spindle-shaped cells, which have the signal-rich interior and signal-poor surrounding (Figs. 4(C, E)). These findings are supported by the corresponding histological image (Fig. 4(E), bottom inset).

With the improved axial and transverse resolutions, the fiber-probe based μ OCT provide a possibility to capture cellular-level microstructures. Compared Figs. 3(B, C) with Figs. 3(B', C'), the microstructures of elastic laminas and smooth muscles can be clearly detected thanks to the enhancement of spatial resolution. Similarly, the cellular and extracellular components such as foam cells and smooth muscle cells can be clearly distinguished, demonstrated by the comparisons between Figs. 4(C-E) to Figs. 4(C'- E').

The current study has a few limitations with respect to a clinically viable technology. First of all, the proposed fiber probe does not have enough axial imaging depth for intravascular imaging *in vivo*. This issue may be resolved by use of DOF extension techniques [30]–[32]. Secondly, we did not include a polymer sheath in our study so that the influence

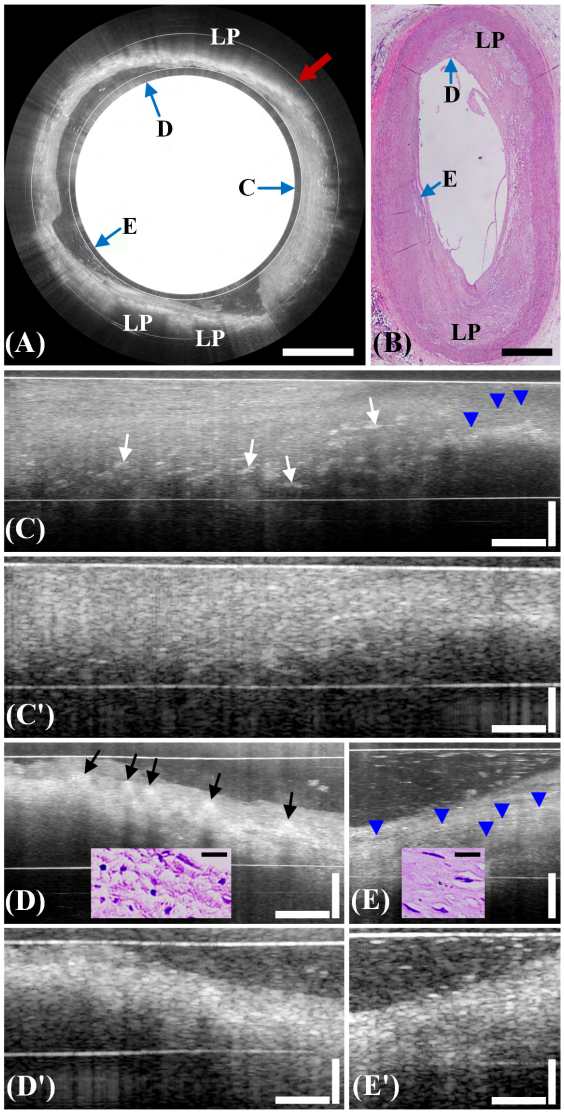

FIGURE 4. Coronary atherosclerotic images acquired by the fiber-probe based μ OCT depicting thickened intima. Human cadaver heart tissue. (A) A representative cross-sectional μ OCT image showing lipid pools as areas with shallow light penetration and graduate decay in the reflectance signal along the radial direction, spindle-shaped foam cells derived from smooth muscle cells (white arrows in (C)), "cotton ball" like foam cells derived from macrophages (black arrows in (D)), and smooth muscle cells (blue arrow heads in (C, E)). It consists of 1024 pixels (axial, 1016.8 μm) × 5184 pixels (circumferential, minimum circle: 8375.5 μm). (B) Corresponding hematoxylin and eosin (H&E) stained histology. Image size of (C): 794.4 μm (axial) × 2036.0 μm (circumferential). Image size of (D): 794.4 μm (axial) × 1252.2 μm (circumferential). Image size of (E): 794.4 μm (axial) × 783.4 μm (circumferential). Insets in (D, E) show representative H&E staining; cell nuclei are stained as dark purple parts; scale bars in H&E insets are 20 μm. (C', D', E') Simulated images by OCT with an axial resolution of ~7 μm in tissue and a transverse resolution of ~20 μm corresponding to the obtained visualizing results in (C, D, E), respectively. LP: lipid pool. Red arrow in (A) indicates the conjugated profile of the inner surface of outer sheath. Scale bars: 1 mm in (A, B); 200 μm in (C-E).

of the polymer sheath on the spatial resolution and sensitivity need to be tested in future. Thirdly, a probe with a smaller size is more available to conduct intravascular imaging, and in the next step, we will adopt a probe with such high resolution and a diameter of less than or equal to 1 mm. Fourthly, we used a relative low imaging speed for image acquisition which is not enough to suppress motion artifacts *in vivo*. The simple solution is to improve the image acquisition.

IV. CONCLUSION

In conclusion, we investigated the feasibility of intravascular imaging by use of a circumferentially scanning μ OCT fiber probe. The results from human atherosclerotic coronary arteries demonstrate the capability of the μ OCT fiber probe to identify key cellular structures in the plaques. Further development of a μ OCT intravascular catheter will provide more accurate assessment of plaque vulnerability and hold promises for the early diagnosis of atherosclerotic lesions.

REFERENCES

[1] H. Wang *et al.*, "Global, regional, and national life expectancy, all-cause mortality, and cause-specific mortality for 249 causes of death, 1980–2015: A systematic analysis for the global Burden of disease study 2015," *Lancet*, vol. 388, no. 10053, pp. 1459–1544, Oct. 2016.
[2] E. Arbustini *et al.*, "Plaque erosion is a major substrate for coronary thrombosis in acute myocardial infarction," *Heart*, vol. 82, no. 3, pp. 269–272, Sep. 1999.
[3] A. C. van der Wal, A. E. Becker, C. M. van der Loos, and P. K. Das, "Site of intimal rupture or erosion of thrombosed coronary atherosclerotic plaques is characterized by an inflammatory process irrespective of the dominant plaque morphology," *Circulation*, vol. 89, pp. 36–44, Jan. 1994.
[4] E. Falk, P. K. Shah, and V. Fuster, "Coronary plaque disruption," *Circulation*, vol. 92, pp. 657–671, Aug. 1995.
[5] R. Virmani, A. P. Burke, A. Farb, and F. D. Kolodgie, "Pathology of the vulnerable plaque," *J. Amer. Coll. Cardiol.*, vol. 47, no. 8, pp. C13–C18, Apr. 2006.
[6] M. J. Davies, P. D. Richardson, N. Woolf, D. R. Katz, and J. Mann, "Risk of thrombosis in human atherosclerotic plaques: Role of extracellular lipid, macrophage, and smooth muscle cell content," *Heart*, vol. 69, no. 5, pp. 377–381, May 1993.
[7] Z. A. Fayad, V. Fuster, K. Nikolaou, and C. Becker, "Computed tomography and magnetic resonance imaging for noninvasive coronary angiography and plaque imaging," *Circulation*, vol. 106, no. 15, pp. 2026–2034, Oct. 2002.
[8] G. A. Rodriguez-Granillo *et al.*, "*In vivo* intravascular ultrasound-derived thin-cap fibroatheroma detection using ultrasound radiofrequency data analysis," *J. Amer. Coll. Cardiol.*, vol. 46, no. 11, pp. 2038–2042, Dec. 2005.
[9] S. G. Carlier and K. Tanaka, "Studying coronary plaque regression with IVUS: A critical review of recent studies," *J. Interv. Cardiol.*, vol. 19, no. 1, pp. 11–15, Feb. 2006.
[10] D. Huang *et al.*, "Optical coherence tomography," *Science*, vol. 254, no. 5035, pp. 1178–1181, 1991.
[11] I.-K. Jang *et al.*, "*In vivo* characterization of coronary atherosclerotic plaque by use of optical coherence tomography," *Circulation*, vol. 111, no. 12, pp. 1551–1555, Mar. 2005.
[12] H. Yoo and J. W. Kim, "Intra-arterial catheter for simultaneous microstructural and molecular imaging *in vivo*," *Nat. Med.*, vol. 17, no. 12, pp. 1680–1684, Dec. 2011.
[13] H. C. Lowe, J. Narula, J. G. Fujimoto, and I.-K. Jang, "Intracoronary optical diagnostics: Current status, limitations, and potential," *JACC, Cardiovascular Intervent.*, vol. 4, no. 12, pp. 1257–1270, Dec. 2011.
[14] W. Drexler, M. Liu, A. Kumar, T. Kamali, A. Unterhuber, and R. A. Leitgeb, "Optical coherence tomography today: Speed, contrast, and multimodality," *J. Biomed. Opt.*, vol. 19, no. 7, pp. 071412-1–071412-34, 2014.
[15] A. Cogliati *et al.*, "MEMS-based handheld scanning probe with pre-shaped input signals for distortion-free images in Gabor-domain optical coherence microscopy," *Opt. Express*, vol. 24, no. 12, pp. 13365–13374, Jun. 2016.
[16] L. Liu *et al.*, "Imaging the subcellular structure of human coronary atherosclerosis using micro–optical coherence tomography," *Nat. Med.*, vol. 17, no. 8, pp. 1010–1014, Aug. 2011.

[17] D. Cui *et al.*, "Dual spectrometer system with spectral compounding for 1-μm optical coherence tomography *in vivo*," *Opt. Lett.*, vol. 39, no. 23, pp. 6727–6730, Dec. 2014.
[18] K. K. Chu *et al.*, "*In vivo* imaging of airway cilia and mucus clearance with micro-optical coherence tomography," *Biomed. Opt. Express*, vol. 7, no. 7, pp. 2494–2505, Jul. 2016.
[19] X. Yu *et al.*, "Toward high-speed imaging of cellular structures in rat colon using micro-optical coherence tomography," *IEEE Photon. J.*, vol. 8, no. 4, pp. 1–8, Aug. 2016.
[20] D. Cui *et al.*, "Flexible, high-resolution micro-optical coherence tomography endobronchial probe toward *in vivo* imaging of cilia," *Opt. Lett.*, vol. 42, no. 4, pp. 867–870, Feb. 2017.
[21] Y. Luo *et al.*, "Endomicroscopic optical coherence tomography for cellular resolution imaging of gastrointestinal tracts," *J. Biophoton.*, vol. 11, no. 4, p. e201700141, Apr. 2018.
[22] W. T. Welford, "Use of annular apertures to increase focal depth," *J. Opt. Soc. Amer.*, vol. 50, no. 8, pp. 749–753, Aug. 1960.
[23] I. W. Selesnick, "The double-density dual-tree DWT," *IEEE Trans. Signal Process.*, vol. 52, no. 5, pp. 1304–1314, May 2004.
[24] A. Zhang, J. Xi, J. Sun, and X. Li, "Pixel-based speckle adjustment for noise reduction in Fourier-domain OCT images," *Biomed. Opt. Express*, vol. 8, no. 3, pp. 1721–1730, Mar. 2017.
[25] S. L. Sandow, D. J. Gzik, and R. M. Lee, "Arterial internal elastic lamina holes: Relationship to function?" *J. Anatomy*, vol. 214, no. 2, pp. 258–266, Feb. 2009.
[26] K. D. O'Brien, D. Gordon, S. Deeb, M. Ferguson, and A. Chait, "Lipoprotein lipase is synthesized by macrophage-derived foam cells in human coronary atherosclerotic plaques," *J. Clin. Investig.*, vol. 89, no. 5, pp. 1544–1550, May 1992.
[27] G. S. Hotamisligil, "Endoplasmic reticulum stress and atherosclerosis," *Nature Med.*, vol. 16, no. 4, pp. 396–399, Apr. 2010.
[28] J. Oh *et al.*, "Endoplasmic reticulum stress controls M2 macrophage differentiation and foam cell formation," *J. Biol. Chem.*, vol. 287, no. 15, pp. 11629–11641, Feb. 2012.
[29] F. D. Kolodgie *et al.*, "Pathologic assessment of the vulnerable human coronary plaque," *Heart*, vol. 90, no. 12, pp. 1385–1391, 2004.
[30] J. Mo, M. de Groot, and J. F. de Boer, "Focus-extension by depth-encoded synthetic aperture in optical coherence tomography," *Opt. Express*, vol. 21, no. 8, pp. 10048–10061, Apr. 2013.
[31] E. Bo *et al.*, "Depth-of-focus extension in optical coherence tomography via multiple aperture synthesis," *Optica*, vol. 4, no. 7, pp. 701–706, Jul. 2017.
[32] B. Yin, C. Hyun, J. A. Gardecki, and G. J. Tearney, "Extended depth of focus for coherence-based cellular imaging," *Optica*, vol. 4, no. 8, pp. 959–965, Aug. 2017.

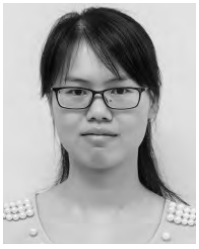

YUEMEI LUO received the B.Eng. degree in mechanical design, manufacturing and automation from the University of Electronic Science and Technology of China in 2011 and the Ph.D. degree from the School of Electrical and Electronic Engineering, Nanyang Technological University, Singapore, in 2018. Her main research focuses on the micro-optical coherence tomography and the endoscopic probes for its clinical applications.

EN BO received the B.Eng. degree in precision instrument from Sichuan University in 2012 and the M.Eng. degree in instrument science and technology from Tianjin University, China, in 2015. He is currently pursuing the Ph.D. degree with Nanyang Technological University, Singapore. His research interests are mainly focused on the development of non-invasive and cellular resolution imaging methods for disease diagnosis using optical coherence tomography.

HAITAO LIANG received the B.Eng. degree in animal medicine from Sichuan Agricultural University in 2012 and the M.Eng. degree in basic veterinary from Huazhong Agricultural University, China, in 2015. He is currently a Research Assistant with Nanyang Technological University, Singapore. His research interests include the development and application of micro-optical coherence tomography in identification of anatomical structures for diagnostic purpose.

XIANGHONG WANG received the master's degree in precision instrument from Tianjin University in 2012. He is currently a Research Associate in electrical and electronic engineering with Nanyang Technological University, Singapore. His research interests include the development of optical coherence tomography instrumentation and biomedical image processing and their applications.

XIAOJUN YU received the Ph.D. degree from Nanyang Technological University, Singapore, in 2015. From 2015 to 2017, he was a Post-Doctoral Research Fellow with Nanyang Technological University. He is currently an Associate Professor with Northwestern Polytechnical University, China. His main research interests include high-resolution optical coherence tomography and its imaging applications.

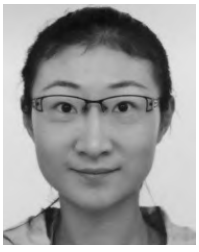

DONGYAO CUI received the B.Eng. and Ph.D. degrees in electrical and electronics engineering from Nanyang Technological University in 2013 and 2018, respectively. Her research interests include the design, development, and validation of advanced micro-optical coherence tomography (μ OCT) systems for high-resolution applications and the development of novel μ OCT endoscopic probes for *in vivo* clinical applications.

XIN GE received the B.S. degree in optics and the Ph.D. degree in synchrotron radiation and its applications from the University of Science and Technology of China in 2008 and 2013, respectively. He is currently a Research Fellow with Nanyang Technological University. His current research interests include high-resolution optical coherence tomography, spectroscopic optical coherence tomography, and related medical applications.

JIANHUA MO received the B.Eng. and M.Eng. degrees from Zhejiang University, Hangzhou, China, and the Ph.D. degree from the National University of Singapore in 2011. He was a Post-Doctoral Fellow with VU University, Amsterdam, The Netherlands, from 2011 to 2013. He is currently an Associate Professor with Soochow University, Suzhou, China. His research interests include optical coherence tomography imaging technique development and its applications in biology and medical diagnostics, and non-destructive inspection in industry.

LINBO LIU received the B.Eng. degree in precision instrument and the M.Eng. degree in optical engineering from Tianjin University, China, in 2001 and 2004, respectively, and the Ph.D. degree in graduate programme in bioengineering from the School of Medicine, National University of Singapore, in 2008. From 2008 to 2011, he completed the post-doctoral training at the Wellman Center in Photomedicine, Harvard Medical School (HMS), Massachusetts General Hospital, where he developed and established a new generation of optical coherence tomography (OCT) technology termed micro-OCT. He was promoted as an Instructor in dermatology at HMS. He joined the School of Electrical and Electronic Engineering and the School of Chemical and Biomedical Engineering,

Nanyang Technological University, as a Nanyang Assistant Professor in 2012.